



Influence of Meteorological Processes on cGPS Measurements of Crustal Movements

Sikelela Gomo*, Gordon R. J. Cooper, Raymond J. Durrheim and Musa S. D. Manzi

School of Geosciences, University of the Witwatersrand, Johannesburg, South Africa

Surface displacement measurements collected using continuous Global Positioning System (cGPS) stations include the contribution of both endogenic processes (e.g., plate tectonics, isostasy) and exogenic processes that show seasonal variation (e.g., climate). These seasonal variations distort the tectonic signals and limit the usefulness of short-term investigations. This paper explores cGPS and meteorological time series collected in southern Africa and investigates whether the usefulness of cGPS time series can be improved by accounting for the seasonal effects of the dominant meteorological processes. The study is carried out using time, frequency, and time-frequency domain signal processing (inferential) analysis techniques. It was found that from the considered atmospheric processes, thermally-induced effects, which are not corrected for in the cGPS data, are the most prominent meteorological contributors in the vertical annual deformation component observed in cGPS time series. The effects of heave action (due to seasonal subsurface water infiltration and absorption, as well as changes in the water table) and changes of water mass distribution (caused by infiltration, transportation, extractions, and evaporation) on the displacement time series are much smaller. This suggests that correcting for thermal expansion, contraction, and thermal-induced errors could reduce the annual seasonal deformation component observed in cGPS position measurements in southern Africa and, most probably, in other parts of the world subjected to large seasonal variations in atmospheric temperatures. Reducing the magnitude of the seasonal components would increase the usefulness of short-term cGPS campaigns.

Keywords: Signal processing, meteorological, cGPS, wavelet, Fourier, semblance, southern Africa

OPEN ACCESS

Edited by:

Mourad Bezzeghoud,
Universidade de Évora, Portugal

Reviewed by:

Yuanjin Pan,
Wuhan University, China
Alexis Rigo,
Laboratoire de géologie de l'Ecole
Normale Supérieure (LG-ENS), France

*Correspondence:

Sikelela Gomo
sikelelagomo@gmail.com

Specialty section:

This article was submitted to
Solid Earth Geophysics,
a section of the journal
Frontiers in Earth Science

Received: 01 December 2021

Accepted: 19 April 2022

Published: 12 May 2022

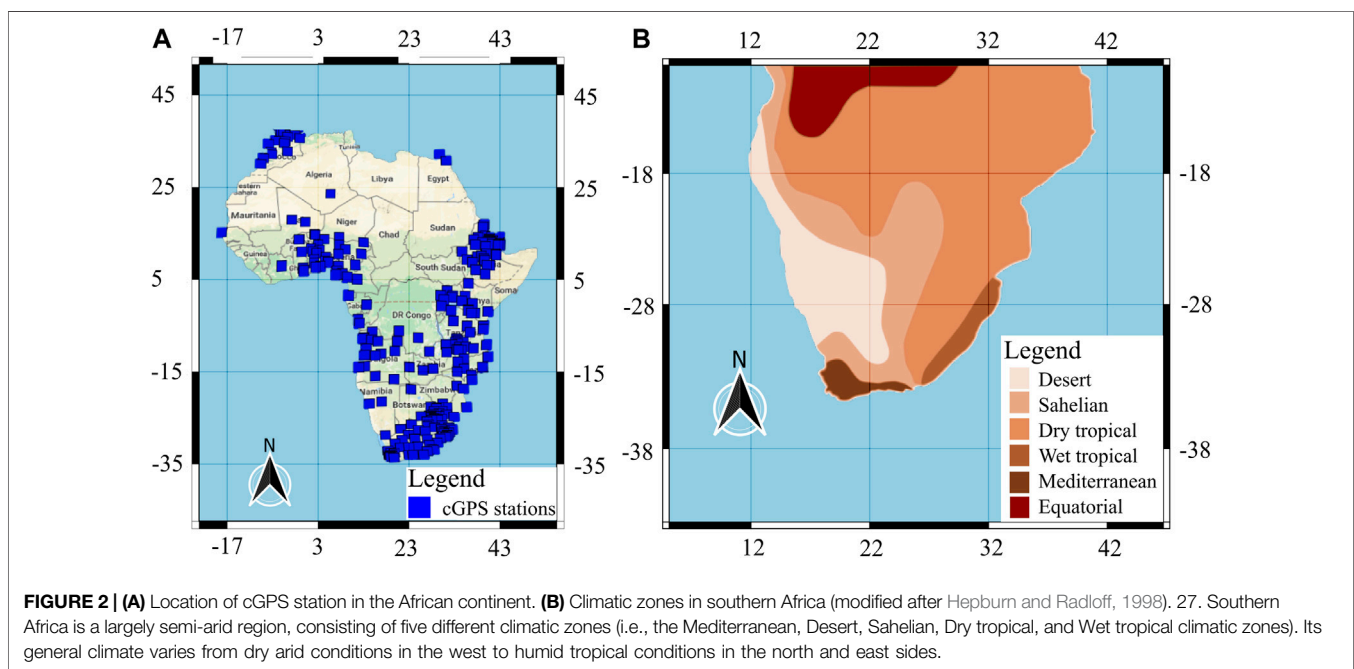
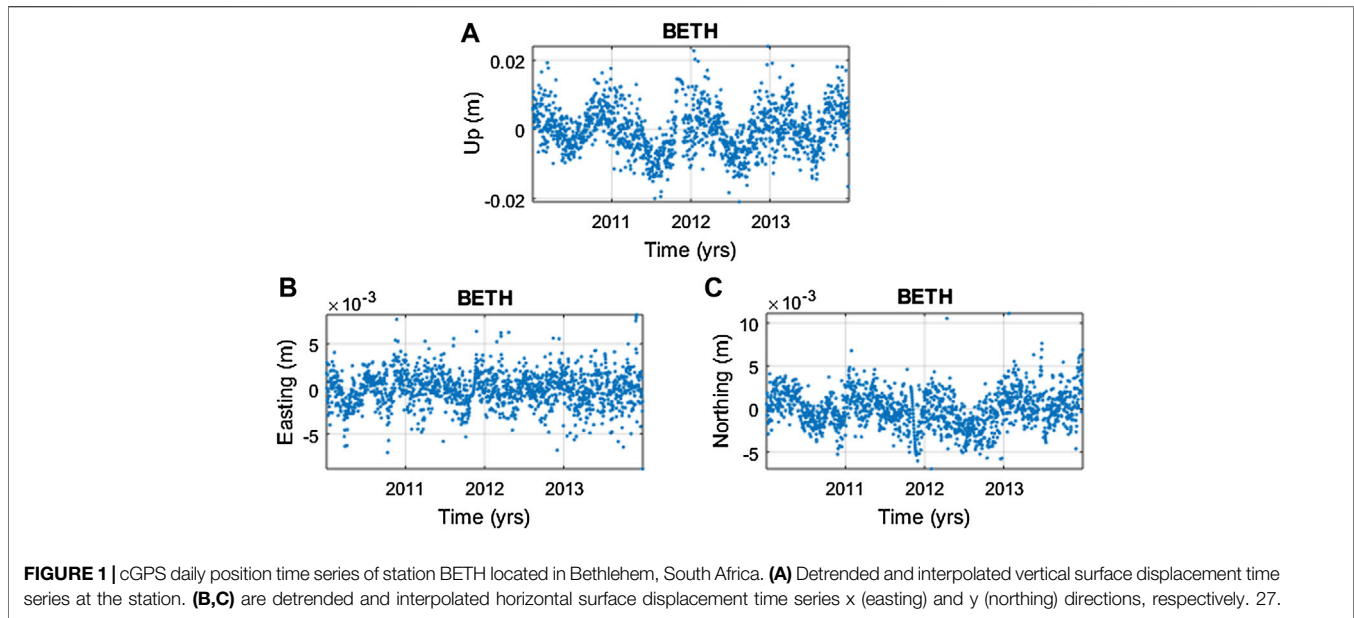
Citation:

Gomo S, Cooper GRJ, Durrheim RJ
and Manzi MSD (2022) Influence of
Meteorological Processes on cGPS
Measurements of Crustal Movements.
Front. Earth Sci. 10:827011.
doi: 10.3389/feart.2022.827011

INTRODUCTION

The continuous Global Positioning System (cGPS) is a space geodetic technique that measures positional changes on the Earth's surface. cGPS measurements are used to study, infer, and monitor plate tectonic motion and drift rates, crustal deformation caused by earthquakes and volcanoes, and crustal motion due to geodynamic and hydrospheric processes (Rabbel and Schuh, 1986; Yan et al., 2009; Argus et al., 2014; Knowles et al., 2020). cGPS data have been used to investigate many space and Earth science research questions, for example, Cilliers et al. (2004) and Malservisi et al. (2013) used the South African cGPS TrigNet network to study the ionospheric conditions over southern Africa, and to investigate the dynamics of the South African portion of the African plate, respectively.

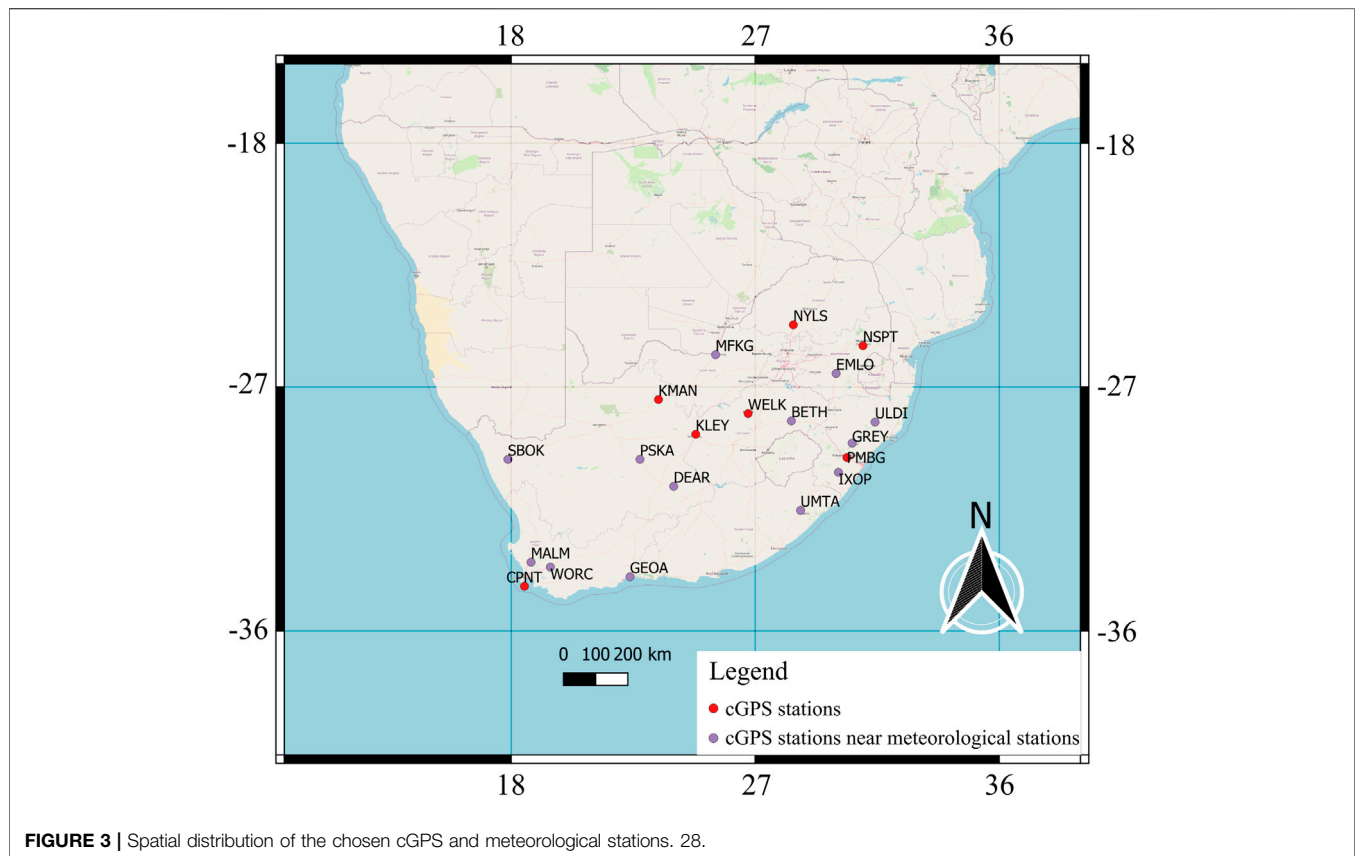
cGPS position measurements generally contain annual and semi-annual seasonal deformation components that are not accounted for and, thus, distort the cGPS measurements (**Figure 1**). Rabbel and Schuh (1986), van Dam and Wahr (1998), and Yan et al. (2009) attribute these deformation



signals to seasonal and partly seasonal variations from multiple sources including surface loading owing to solid Earth tides, pole tides, oceanic tides, atmospheric mass variations, and non-tidal surface fluctuations. Moreover, processing- and equipment-induced errors contribute to the observed seasonal variations. Thermal expansion and contraction of the cGPS monument and the bedrock, along with soil consolidation and the extraction of surface and subsurface water mass near a cGPS station are also thought to be significant contributors of local surface deformation signals (van Dam et al., 2001; Romagnoli et al., 2003; Yan et al., 2009). The vertical displacement of these seasonal deformation components tends to be largest as some exogenic

processes (e.g., atmospheric loading and oceanic loading) induce greater surface displacement in the vertical direction than in the horizontal direction (**Figure 1**) (Dong et al., 2002; Min et al., 2005; He et al., 2015).

This study sought to better understand cGPS and meteorological data collected in southern Africa and draw inference on the seasonal influence of meteorological processes and climatic zones on the vertical component of cGPS surface displacement measurements. This study is fitting, as in some areas (e.g., the Amazon basin) mass loading has been demonstrated to be driven by its local climatic system, and cGPS measurements have been observed to have high enough



temporal resolution to enable the correlation of cGPS measurements and that of several other environmental parameters (Romagnoli et al., 2003; Davis et al., 2004; Yan et al., 2009; Fu et al., 2013; Knowles et al., 2020). Additionally, Knowles et al. (2020) suggest that cGPS time series record displacements are driven by local- and large-scale climate oscillations. Southern Africa is an ideal place to conduct such research because it has several well-maintained cGPS (Figure 2A) and meteorology stations, situated in regions of varying climatic zones (Figure 2B), and low seismic and tectonic activity.

MATERIALS AND METHODS

Description

In this paper, we used data from the South African TrigNet geodetic network and the South African Weather Service (SAWS) to investigate the seasonal effects of changing atmospheric temperature, pressure, rainfall, and humidity processes on vertical cGPS surface displacement measurements. The cGPS data are archived and processed by the geodetic laboratory at the University of Nevada Reno (UNR) (<http://geodesy.unr.edu/index.php>) (Blewitt et al., 2018). The data processing is based on the International GNSS Service (IGS14) realization of the International Terrestrial Reference Frame 2014 (ITRF14) (Altamimi et al., 2016; Rebischung et al., 2016). The processing by UNR includes corrections for tropospheric

effects (i.e., hydrostatic and non-hydrostatic delays), first-order ionospheric effects, solid Earth tides, pole tides, and oceanic tide loading. However, it does not include corrections for non-tidal loading effects (e.g., atmospheric pressure, ocean bottom pressure, surface hydrology), seasonal thermal expansion, and shrink-swell heave effects. The complete processing procedure of the cGPS dataset is given at <http://geodesy.unr.edu/gps/ngl.acn.txt>. The meteorological data used are from meteorological ground stations managed by the SAWS. To be able to analyse the data for annual and semi-annual seasonal variation, both the cGPS and meteorological data were corrected for long term tectonic and climatic variations by detrending the data. In preparing the data for spectral analysis, the data were detrended, zero centred, interpolated and windowed to minimise the occurrence of spectral distortion, leakage, shift, and the formation of false peaks.

All the data used for the study were acquired in South Africa (Figure 3) because 1) most of the cGPS stations in southern Africa are in South Africa; and 2) the cGPS data from other southern African countries have many gaps, which makes it difficult to apply signal processing techniques. Our results are expected to be valid in other southern African regions as the environmental setting is similar.

Analysis Techniques

Inferential signal processing techniques were used to explore the nature of the chosen cGPS and meteorological datasets and to infer their relationships. The time series were decomposed and

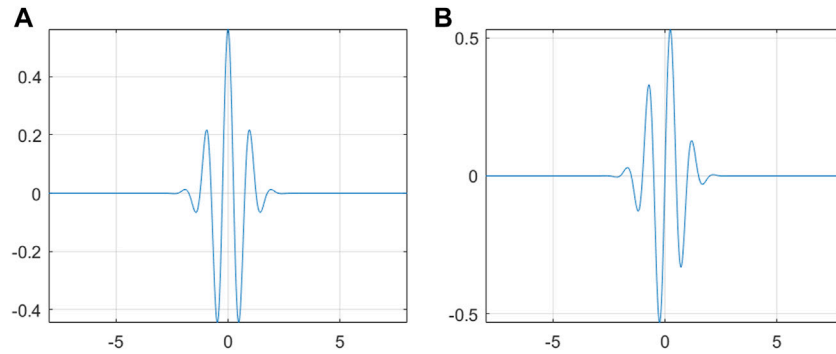


FIGURE 4 | (A) Real part of the complex Morlet wavelet and **(B)** Imaginary part of the complex Morlet wavelet. 28.

correlated in the time, frequency, and time-frequency domains. The various analysis techniques are briefly described below.

Spearman's correlation coefficient (ρ) is a nonparametric (distribution free) rank correlation time domain technique defined as (Gauthier, 2001; Mukaka, 2012):

$$r_s = 1 - \frac{6 \sum_{i=1}^n d_i^2}{n(n^2 - 1)} \quad (1)$$

where d_i is the difference in rank for each continuous variable pair $x(t)$ and $y(t)$, while n is the total number of continuous variable pairs (Mukaka, 2012). The technique is used because it is not affected by outliers, nor assume linearity and normality (Gauthier, 2001).

The Fourier Transform (FT) is a frequency domain decomposition technique used in this study to uncover the dominant frequency components of the cGPS and meteorological time series. The FT $X(f)$ of a time series $x(t)$ is defined as (Cooper and Cowan, 2008; Mallat, 2009):

$$X(f) = \int_{-\infty}^{\infty} x(t) e^{-2\pi i f t} dt \quad (2)$$

where f is the frequency of the time series, i is the imaginary unit, $x(t)$ is the dataset to be analyzed, and t is the time. In this study, Fourier analysis is implemented using the Fast Fourier Transform (FFT), which is an efficient technique for implementing the discrete Fourier transform (DFT) (Cochran et al., 1967; Mallat 2009; Trauth, 2010; Ryan, 2015). The Welch periodogram was used to produce the power spectrum of the datasets and the FFT was used to compute the amplitude of the time series (Warner, 1998).

The magnitude-squared coherence (MSC) is a complex frequency domain technique used in this study to determine and quantify the relationship strength of the components of the cGPS and meteorological time series in the frequency domain (Torrence and Compo, 1998; Friston et al., 2011). The technique is mathematically defined as:

$$C_{xy} = \frac{|X_{xy}(f)|^2}{X_{xx}(f)X_{yy}(f)} \quad (3)$$

where X_{xy} is the cross-power spectral density of time series $x(t)$ and $y(t)$, $X_{xx}(f)$ and $X_{yy}(f)$ are the power spectral densities of $x(t)$ and $y(t)$, and C_{xy} is the coherence (Friston et al., 2011).

The continuous wavelet transform (CWT) is a time-frequency domain decomposition technique used in this study to decompose the cGPS and meteorological time series. The CWT is good at analyzing both continuous and discrete time series; unlike the FT, it is also good at decomposing non-stationary time series (Zhao et al., 2004; Baker, 2007; Kaiser, 2011). The CWT is mathematically defined as (Mallat, 1998, p. 5):

$$\text{CWT}(u, s) = \int_{-\infty}^{\infty} f(t) \frac{1}{|s|^{0.5}} \psi^* \left(\frac{t-u}{s} \right) dt, \quad (4)$$

where s and u are the scale and translation (position) factors, respectively, $f(t)$ is the time domain function being decomposed, ψ is the mother wavelet and $*$ means complex conjugate (Meyers et al., 1993; Cooper and Cowan, 2008). The method decomposes a time series at multiple scales using a linear combination of translated and dilated daughter wavelets, which enable it to easily map temporal variations in the spectral characteristics of a time series over time (Graps, 1995; Torrence and Compo, 1998; Baker, 2007; Cooper and Cowan, 2008; Fletcher and Sangwine, 2017). However, it is unable to obtain precise measurements of both frequency and time, as the technique has a trade-off between the accuracy in time and frequency as dictated by the uncertainty principle (Issartel et al., 2015). The complex Morlet wavelet transform was used in this study because of its nonorthogonality, similarity to the cGPS and meteorological time series, as well as for its high degree of smoothing (Torrence and Compo, 1998; Struzik, 2001; Mallat, 2009) (Figure 4). The complex Morlet wavelet transform is defined as (Teolis, 1998, p. 66):

$$\psi_o(x) = \frac{1}{\pi f_b} e^{2\pi i f_c x} e^{-x^2/f_b} \quad (5)$$

where f_b is the bandwidth parameter, i is the imaginary unit and f_c is the wavelet centre frequency. A centre frequency and bandwidth value of one was used to compute the wavelet transform, so as to make the used scales equivalent to the

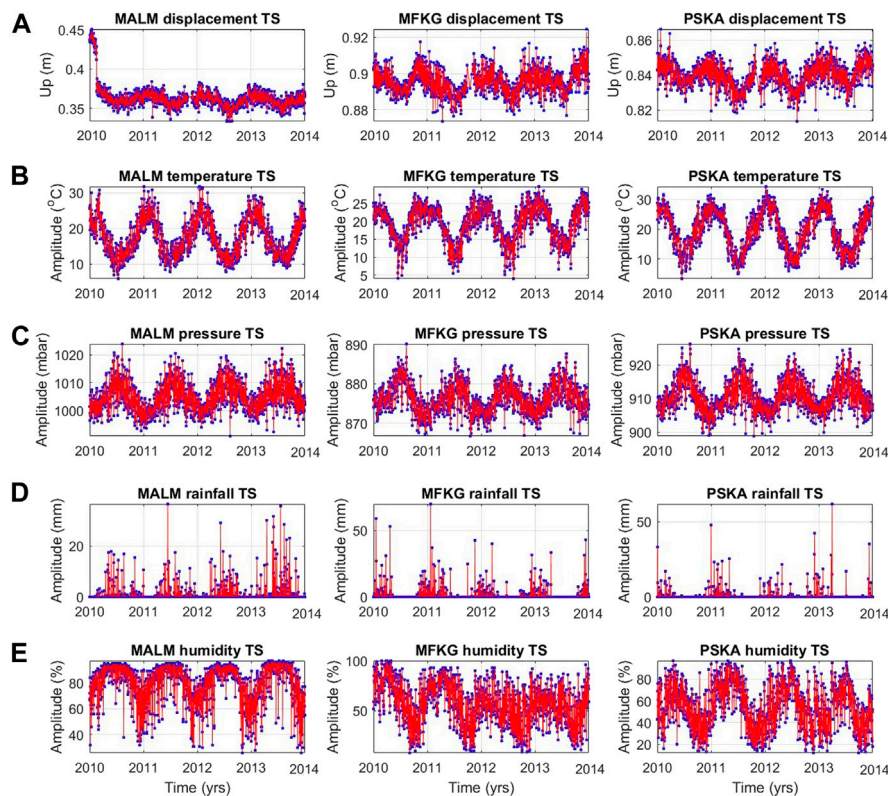


FIGURE 5 | Time domain displacement and meteorological time series at stations MALM, MFKG, and PSKA situated in the towns of Malmesbury, Mahikeng, and Prieska, respectively, the station names are the abbreviations of the town names where they are located. **(A)** cGPS surface displacement, **(B)** atmospheric temperature, **(C)** atmospheric pressure, **(D)** rainfall, and **(E)** humidity time series across stations in southern Africa. Due to a lack of space and similarity of the results, results for only three stations are shown. 29.

wavelength (Cooper and Cowan, 2008), which is also an inverse of frequency.

The wavelet-based semblance (WS) is a qualitative time-frequency domain technique used in this study to correlate the cGPS and meteorological time series in the time-frequency domain. Since the method uses phase information, it can be used to compute the correlation of time series with different units of measure and is mathematically defined as (Christensen, 2003; Cooper, 2009).

$$S = \cos^n(\theta) \quad (6)$$

where n is an odd integer greater than zero, that allows the response of the technique to be refined, in this paper, $n = 1$ was used to compute the semblance results, while θ refers to the local phase of the time series.

RESULTS AND INTERPRETATION

FFT and CWT Decomposition Analysis Surface Displacement

Frequency and time-frequency domain decomposition results show that surface displacement time series consist of an

annual and semi-annual deformation component (Figures 5A, 6A, 7A, Supplementary Material Appendix 1, Figures 1, 2, 3). The power of the annual displacement component is larger than that of the semi-annual component at most stations, often by one order of magnitude (Table 1). This is consistent with the findings in other areas of the world (Ray et al., 2008). The power of the time series varies systematically between the different climatic zones (Table 1). This implies that the magnitude of seasonal weather variation within a climatic zone has an influence on the magnitude of the deformation components observed in the surface displacement time series. The annual displacement components are largest in cGPS data from the Desert climatic zone and lower in time series at stations located in the Wet and Dry Tropical climatic zones (Table 1). The CWT spectrums show slight variation in cycle periods and frequency (non-stationarity) of the time series over time, this is characteristic of signals in the real environment (Figure 7).

Atmospheric Temperature

Atmospheric temperature time series are predominantly composed of an annual and semi-annual seasonal component. (Figures 5B, 6B, 7B, Supplementary Material Appendix 2, Figures 4, 5, 6). The semi-annual component is absent in the

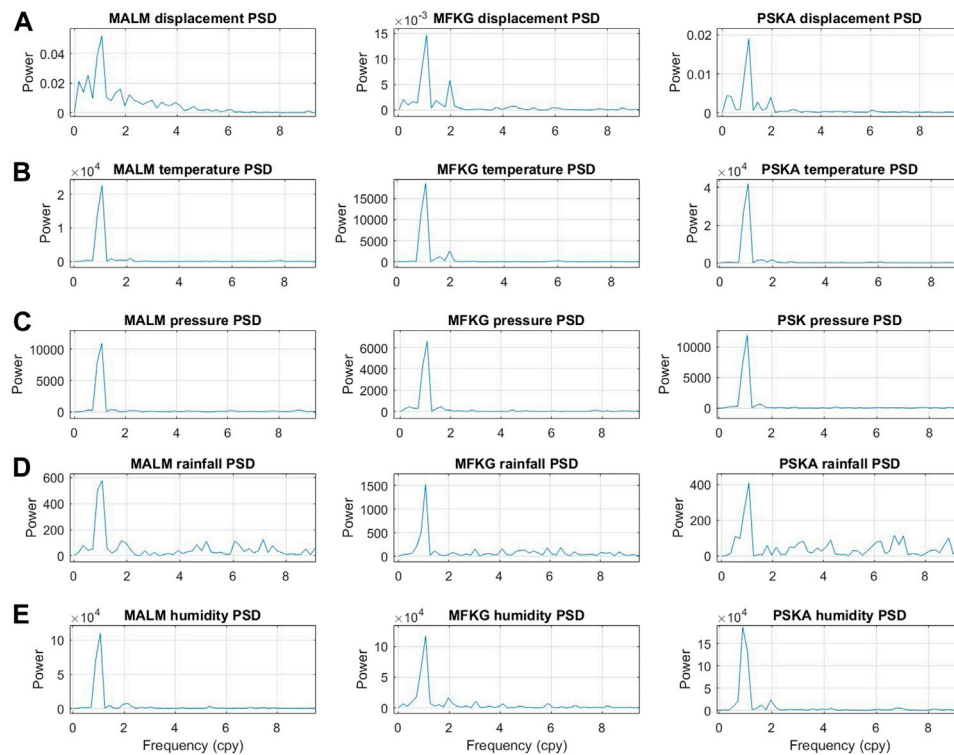


FIGURE 6 | Fourier power spectra. **(A)** cGPS surface displacement, **(B)** atmospheric temperature, **(C)** atmospheric pressure, **(D)** rainfall, and **(E)** humidity decomposition spectra. 30.

temperature time series in the Mediterranean climatic zone. The temperature time series are also characterised by a low noise level and a high degree of stationarity (Figures 6B, 7B, Supplementary Material Appendix 2, Figures 4, 5, 6). Annual seasonal temperature fluctuations are higher in time series from the Desert and Sahelian climatic zones, regions where the Intertropical Convergence Zone (ITCZ) does not move over, and lower in time series from the Dry and Wet Tropical climatic zones - regions where the ITCZ passes over (Table 2). This is because areas characterised by low levels of cloudiness are characterised by high temperatures and extreme seasonal temperature fluctuation, while areas of high cloudiness are characterised by low temperatures and low-temperature fluctuation, except during tropical storms (Hobbs et al., 1998; Barry and Chorley, 2010).

Atmospheric Pressure

Atmospheric pressure time series consist only of the annual seasonal component (Figures 5C, 6C, 7C, Supplementary Material Appendix 2, Figures 7, 8, 9). The time series are characterised by low levels of noise, variance, spectral averaging, and a high degree of stationarity (Figures 6C, 7C). Seasonal atmospheric pressure fluctuations are higher at stations from the Desert and Mediterranean climatic zones and lower at stations from the Wet and Dry Tropical

climatic zones (Table 2). This is because subtropical deserts are high seasonal atmospheric pressure zones due to the seasonal presence of Hadley cells over them, and tropical climatic regions are low atmospheric pressure fluctuation zones (Nicholson and Flohn, 1980; Barry and Chorley, 2010; Bollasina and Nigam, 2010). Insolation differences due to the absence and presence of clouds in the Desert and Tropical climatic zones, respectively, may also play a role.

Rainfall

Rainfall time series predominantly consist of an annual seasonal component only, the phase of the annual component varies moving across the central, north-eastern, and south-western parts of southern Africa (Figures 5D, 6D, 7D, Supplementary Material Appendix 2, Figures 10, 11, 12). The time series are characterised by a high degree of noise and variance, which, according to Potter and Colman (2003), Jury (2013) and MacKellar et al. (2014) is caused by processes, such as the ITCZ, solar radiation, El Niño-Southern Oscillation (ENSO), and variations in atmospheric circulation. Seasonal rainfall fluctuations are higher in time series from the Wet and Dry Tropical climatic zones and low in time series from the Desert climatic zone (Table 2). These findings are consistent with known information, i.e., continental Dry and Wet Tropical climatic zones are characterised by well-defined alternating high

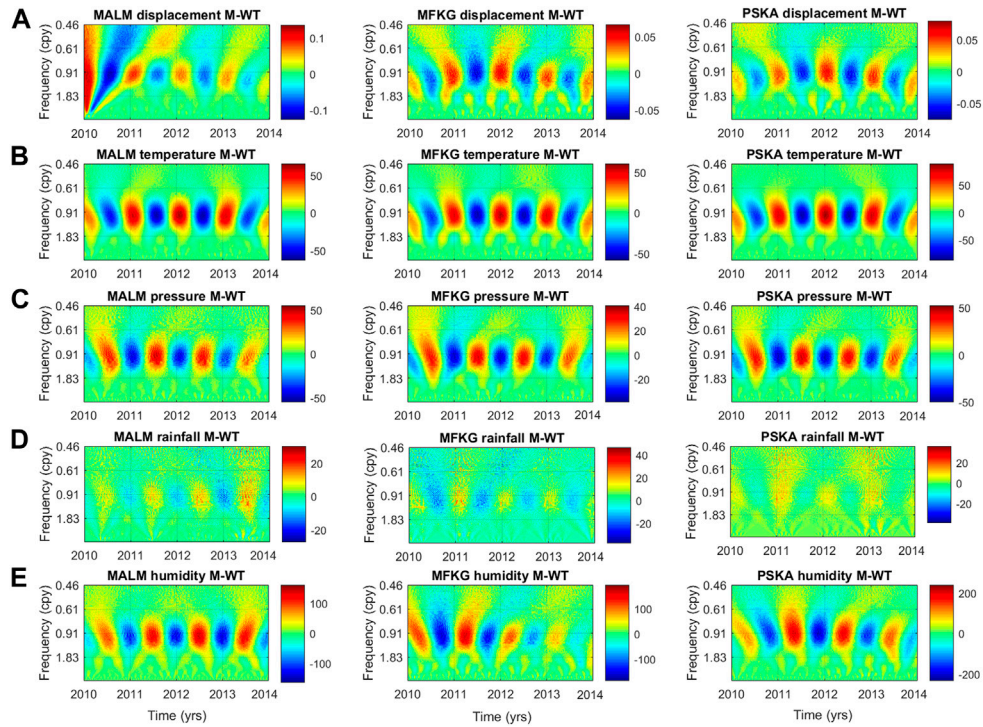


FIGURE 7 | Wavelet Transform (WT) decomposition spectra. **(A)** cGPS surface displacement, **(B)** atmospheric temperature, **(C)** atmospheric pressure, **(D)** rainfall, and **(E)** humidity decomposition spectra. Some of the characteristic CWT features observed in the plots are the exaggeration of low frequencies, suppression of high frequencies, and component frequency overlap. The spectra are also characterised by good time localisation. 31.

TABLE 1 | Climatic zone, latitude longitude, power, and amplitude of the analysed cGPS station, displacement time series.

Station name	Climatic zone	Latitude	Longitude	Percentage of at hand data points (%)	Interpolation technique (linear <95%> Cubic)	Variance (Time domain)	Power		Amplitude (m)	
							Annual component	Semi-annual component	Annual component	Semi-annual component
KMAN	Desert	-27.461	23.432	99	Cubic Hermite	0.0000594	0.0225	0.0029	0.0048	0.0010
PSKA	Desert	-29.668	22.749	93	Linear	0.0000511	0.0155	0.0031	0.0054	0.0019
SBOK	Desert	-29.669	17.879	94	Linear	0.0000504	0.0174	0.0036	0.0054	0.0022
PMBG	Wet Tropical	-29.601	30.383	95	Cubic Hermite	0.0000487	0.0109	0.0031	0.0039	0.0014
ULDI	Wet Tropical	-28.293	31.421	90	Linear	0.0000456	0.0049	0.0008	0.0027	0.0010
GREY	Wet Tropical	-29.071	30.578	92	Linear	0.0000468	0.0078	0.0014	0.0044	0.0007
IXOP	Wet Tropical	-30.146	30.069	95	Cubic Hermite	0.0000740	0.0143	0.0023	0.0054	0.0008
UMTA	Wet Tropical	-31.549	28.673	85	Linear	0.0000363	0.0025	0.0011	0.0019	0.0014
KLEY	Sahelian	-28.743	24.806	99	Cubic Hermite	0.0000564	0.0189	0.0039	0.0048	0.0016
DEAR	Sahelian	-30.665	23.993	93	Linear	0.0000457	0.0146	0.0028	0.0051	0.0019
WELK	Sahelian	-27.978	26.738	99	Cubic Hermite	0.0000398	0.0074	0.0026	0.0029	0.0008
MFKG	Sahelian	-25.805	25.540	93	Linear	0.0000457	0.0121	0.0047	0.0049	0.0026
BWES	Sahelian	-33.347	22.574	98	Cubic Hermite	0.0000539	0.0146	0.0021	0.0030	0.0010
EMLO	Dry Tropical	-26.498	29.984	93	Linear	0.0000421	0.0077	0.0018	0.0038	0.0016
BETH	Dry Tropical/ Sahelian	-28.250	28.334	96	Cubic Hermite	0.0000455	0.0119	0.0033	0.0047	0.0022
NSPT	Dry Tropical	-25.475	30.975	99	Cubic Hermite	0.0000483	0.0066	0.0031	0.0037	0.0013
NYLS	Dry Tropical	-24.703	28.406	98	Cubic Hermite	0.0000530	0.0098	0.0041	0.0038	0.0014
CPNT	Mediterranean	-34.353	18.490	97	Cubic Hermite	0.0000426	0.0035	0.0033	0.0018	0.0013
MALM	Mediterranean	-33.464	18.731	96	Cubic Hermite	0.0002089	0.0468	0.0063	0.0102	0.0026
GEOA	Mediterranean	-34.002	22.383	94	Linear	0.0000350	0.0041	0.0013	0.0029	0.0012
WORC	Mediterranean	-33.645	19.445	93	Linear	0.0000803	0.0223	0.0029	0.0064	0.0019

TABLE 2 | Quantified power of the annual and semi-annual frequency components forming the meteorological time series as obtained from FFT.

Climatic Zones	GPS Station Name	Annual and Semi-annual Power of the cGPS Vertical Component Time Series							
		Temperature		Pressure		Rainfall		Humidity	
		Annual	Semi-annual	Annual	Semi-annual	Annual	Semi-annual	Annual	Semi-annual
Desert	PSKA	36,021	1,360	10,098	101	350.7	14.2	154,380	20,240
	SBOK	17,539	993	4,560.5	29.5	58.1	22.3	29,000	5,235
	KMAN	—	—	—	—	—	—	—	—
Wet Tropical	GREY	11,577	1,174	4,281	111.3	1,052.5	47.7	13,597	1,215
	UMTA	8,794	926.4	2,740.7	629.2	—	—	9,656.3	905.3
	IXOP	19,476	1,349	4,115.8	127.2	1,169	43.3	10,573	1,131
	ULDI	7,886	768	5,645	131	1885.5	94.5	20,085	845
	PMBG	—	—	—	—	—	—	—	—
Sahelian	DEAR	26,648	1,103	—	—	735	69.8	103,010	14,440
	MFKG	15,758	2063	5,709.4	107.9	1,120	37.4	96,145	14,339
	KLEY	—	—	—	—	—	—	—	—
	WELK	—	—	—	—	—	—	—	—
Dry Tropical	EMLO	10,292	1,277	1,438.6	46.6	1921.3	22.8	—	—
	BETH	20,424	1,581	2,169.8	277.7	2,661.6	403.7	—	—
	NSPT	—	—	—	—	—	—	—	—
	NYLS	—	—	—	—	—	—	—	—
Mediterranean	MALM	19,301	390	9,728.5	61	548.5	87.67	95,412	6,597
	GEOA	6,782	40.7	3,989.7	51.4	142.7	31.3	2,930.4	4,990.3
	WORC	—	—	6,843.7	47.7	328.1	51.1	62,707	1889
	CPNT	—	—	—	—	—	—	—	—

rainfall and dry seasons (Hepburn and Radloff, 1998; Barry and Chorley, 2010).

Humidity

Humidity data consist of an annual and semi-annual seasonal component, except for stations in the Wet Tropical climatic zone (Figures 5E, 6E, 7E, Supplementary Material Appendix 2, Figures 13, 14, 15). The phase of the humidity time series varies as a function of time and spatial geographic location, similar to rainfall time series but less defined. In general, in the central and north-eastern parts of southern Africa, the moisture content is high during summer and low during winter; while in the south-western parts of southern Africa, humidity levels are high during winter and low during summer. It is important to note that at some stations (e.g., PSKA), a deviation is observed from this general trend. It is also observed that humidity fluctuations are greater in the semi-arid regions than in tropical regions, which could be because annual humidity fluctuation is more defined in the semi-arid region than in the tropics.

Correlation Analysis

The time, frequency, and time-frequency domain comparisons show that surface displacement is directly and inversely proportional to atmospheric temperature and pressure changes, respectively. The correlation between atmospheric temperature, pressure, and surface displacement is highest in stations in the Desert, Sahelian, and Mediterranean climatic zones (Tables 3, 4), these are zones that receive the

most solar radiation, heat, and least amount of water in southern Africa. The displacement-temperature correlation is observed to be smallest in the Dry and Wet Tropical climatic zones, which are climatic zones that are cooler and receive the most amounts of rainfall. In addition, the frequency and phase correlation results between surface displacement-temperature and surface displacement-pressure time series show a high and consistent frequency and phase correlation

TABLE 3 | Displacement time series correlation values with atmospheric temperature (T), atmospheric pressure (P), rainfall (R), and humidity (H) time series at the selected stations in southern Africa.

Climatic Zones	cGPS Station Name	Spearman's Correlation (Rho)			
		T	P	R	H
Desert	PSKA	0.59	-0.40	0.09	-0.35
	SBOK	0.65	-0.27	-0.16	-0.44
Sahelian	DEAR	0.61	—	0.05	-0.34
	MFKG	0.57	-0.39	0.17	-0.10
Mediterranean	MALM	0.59	-0.28	-0.42	-0.34
	GEOA	0.47	-0.22	-0.05	-0.01
	WORC	0.50	0.02	-0.21	-0.16
Dry tropical	EMLO	0.43	-0.32	0.12	—
	BETH	0.51	-0.28	0.22	—
Wet tropical	GREY	0.38	-0.19	0.11	-0.09
	UMTA	0.33	-0.31	—	-0.19
	IXOP	0.41	-0.10	-0.02	0.00
	ULDI	0.30	-0.26	0.10	-0.03

TABLE 4 | Coherence correlation strength of displacement vs. meteorological (average temperature, pressure, rainfall, and humidity) processes.

Climatic Zones	GPS Station Name	Coherence Spectral Correlation (Vertical Component of Displacement vs. Atmospheric Processes)							
		Temperature		Pressure		Rainfall		Humidity	
		Annual	Semi-annual	Annual	Semi-annual	Annual	Semi-annual	Annual	Semi-annual
Desert	PSKA	0.92	0.90	0.89	0.24	0.75	0.31	0.99	-
	SBOK	0.99	0.56	0.95	0.13	0.42	0.30	0.91	0.36
Sahelian	DEAR	0.91	0.73	—	—	0.75	0.35	0.97	0.97
	MFKG	0.92	0.96	0.87	0.42	0.73	0.97	0.78	0.86
Mediterranean	MALM	0.99	0.21	0.98	0.59	0.98	0.31	0.99	0.08
	GEOA	0.87	0.85	0.83	0.88	0.77	0.37	0.79	0.94
	WORC	0.99	0.86	0.98	0.19	0.99	0.72	1.00	0.92
Dry Tropical	EMLO	0.89	0.79	0.86	0.13	0.88	0.03	—	—
	BETH	0.90	0.84	0.87	0.28	0.77	0.81	—	—
Wet Tropical	GREY	0.75	0.58	0.70	0.11	0.60	0.24	0.44	0.41
	UMTA	0.95	0.86	0.93	0.73	—	—	0.72	0.68
	IXOP	0.84	0.73	0.80	0.39	0.78	0.18	0.59	0.52
	ULDI	0.89	0.65	0.86	0.76	0.92	0.95	0.72	0.40
Annual average		0.91	-	0.88	—	0.76	—	0.81	—
Semi-annual average		0.72	—	0.40		0.44		0.61	
STD annual		0.07		0.08		0.16		0.18	
STD semi-annual			0.20		0.27		0.32		0.31

between the time series (Figures 8A,8B, 9A,9B, Supplementary material Appendix 3: Figures 16, 17).

Depending on the spatial location, rainfall and humidity time series are either directly or inversely correlated to surface displacement time series. The correlation of the time series is low in the time domain, that of the annual component is high to moderate in the frequency and time-frequency domains (Tables 3, 4; Figures 8C, D, 9C, D, Supplementary Material Appendix 3: Figures 16, 17). The displacement-rainfall and displacement-humidity correlation, at certain locations, is observed to be inconsistent over time (Figure 9).

The relation between the semi-annual component of the temperature and humidity time series with that of the cGPS surface displacement is too inconsistent to suggest that any of the considered meteorological processes have an influence, if at all, on the semi-annual deformation components (Table 4) (Figure 8).

DISCUSSION

Meteorological Time Series

The temperature, pressure, rainfall, and humidity fluctuations in southern Africa are primarily controlled by the complex interaction between midlatitude, tropical, and subtropical climate systems, together with the development, seasonal positional-shift, and interaction of atmospheric and oceanic circulation systems of the Atlantic, Indian, and Southern oceans (Chase and Meadows, 2007). This is apparent in the temperature and pressure data in southern Africa, which

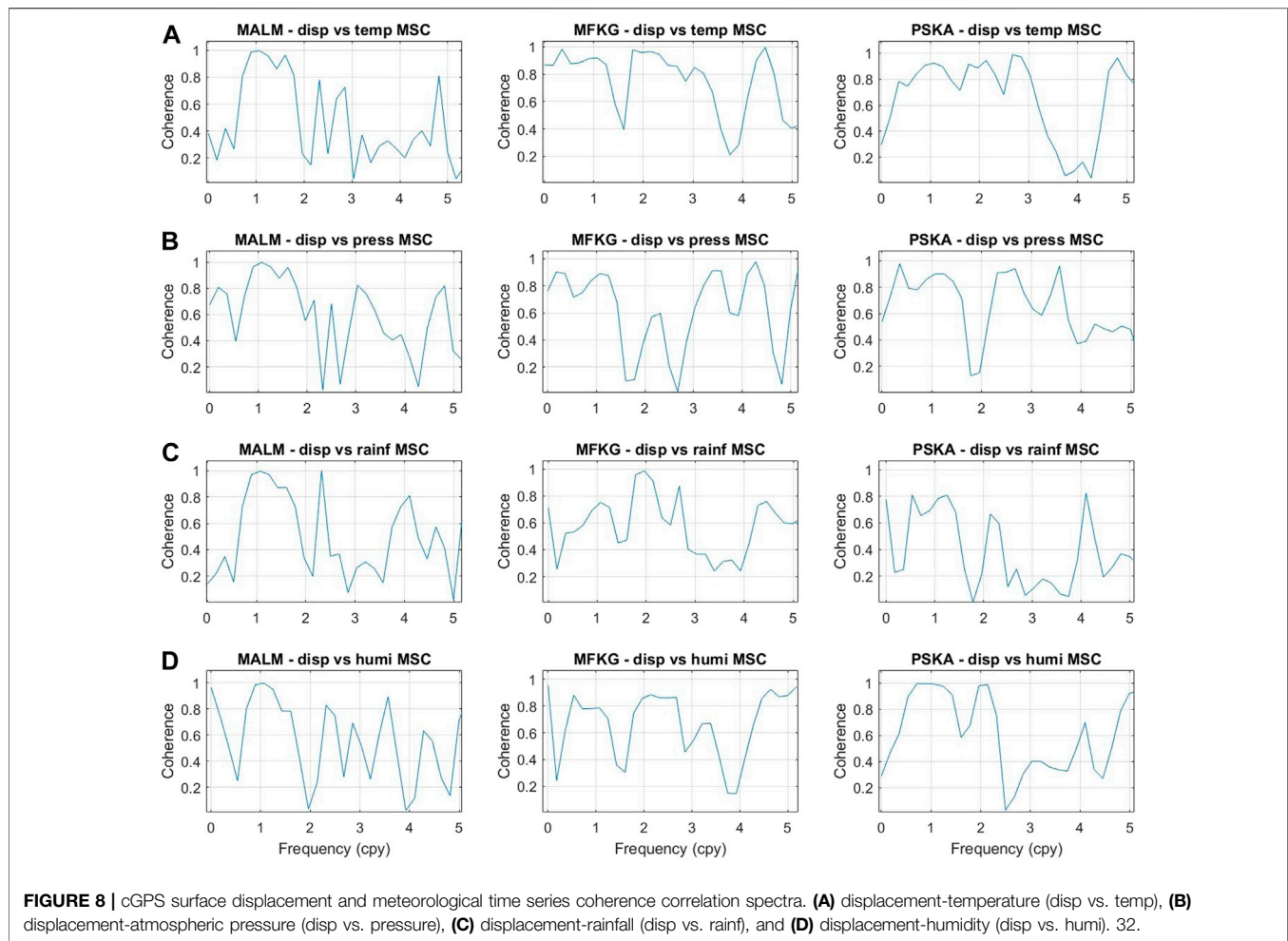
appear to be controlled by 1) the seasonal variation in the Sun's radiation, 2) migration of the ITCZ away from the southern hemisphere (after summer periods) to the northern hemisphere, and 3) a shift of anticyclones from the southern Atlantic and Indian oceans towards the southern Africa continent in winter (Hobbs et al., 1998; Sun et al., 2017; Byrne et al., 2018).

The ITCZ is also the primary source of rainfall activity in the central and north-eastern parts of southern Africa, thus these regions are summer rainfall regions. In the south-western parts of southern Africa, rainfall is associated with the winter inflow of low- and high-level westerlies that carry moist air (Ellis and Galvin, 1994; Barry and Chorley, 2010).

Moist air, in the central and north-eastern parts of southern Africa, is brought by inflowing easterlies that carry moist air from the southwest Indian Ocean and warm Agulhas currents (Chase and Meadows, 2007; Jury, 2013). In the south-western parts of southern Africa, moist air is brought about by westerlies as they move towards the equator during winter (Chase and Meadows, 2007).

Displacement Time Series

Similar to the studies conducted by Dong et al. (2002) and Ray et al. (2008), using a global dataset and Earth model, cGPS displacement time series in southern Africa are found to consist of two dominant seasonal components. Dong et al. (2002), Romagnoli et al. (2003) and Xu et al. (2017) link these deformation components to gravitational attraction, thermal, hydrodynamical, unmodeled, and error-related processes. The observed systematic variation of the power of the displacement



time series suggests that the magnitude of seasonal weather variation within a climatic zone has an influence on the magnitude of the deformation components observed in the cGPS surface displacement time series. It indicates that changes in atmospheric temperature, atmospheric pressure, rainfall, and humidity processes in each climatic zone do have an influence on the surface deformation recorded by cGPS station. These findings demonstrate the influence of local effects on cGPS measurements, which is consistent with what has been found in other studies (Romagnoli et al., 2003; Nahmani et al., 2012; Fu et al., 2013; Knowles et al., 2020).

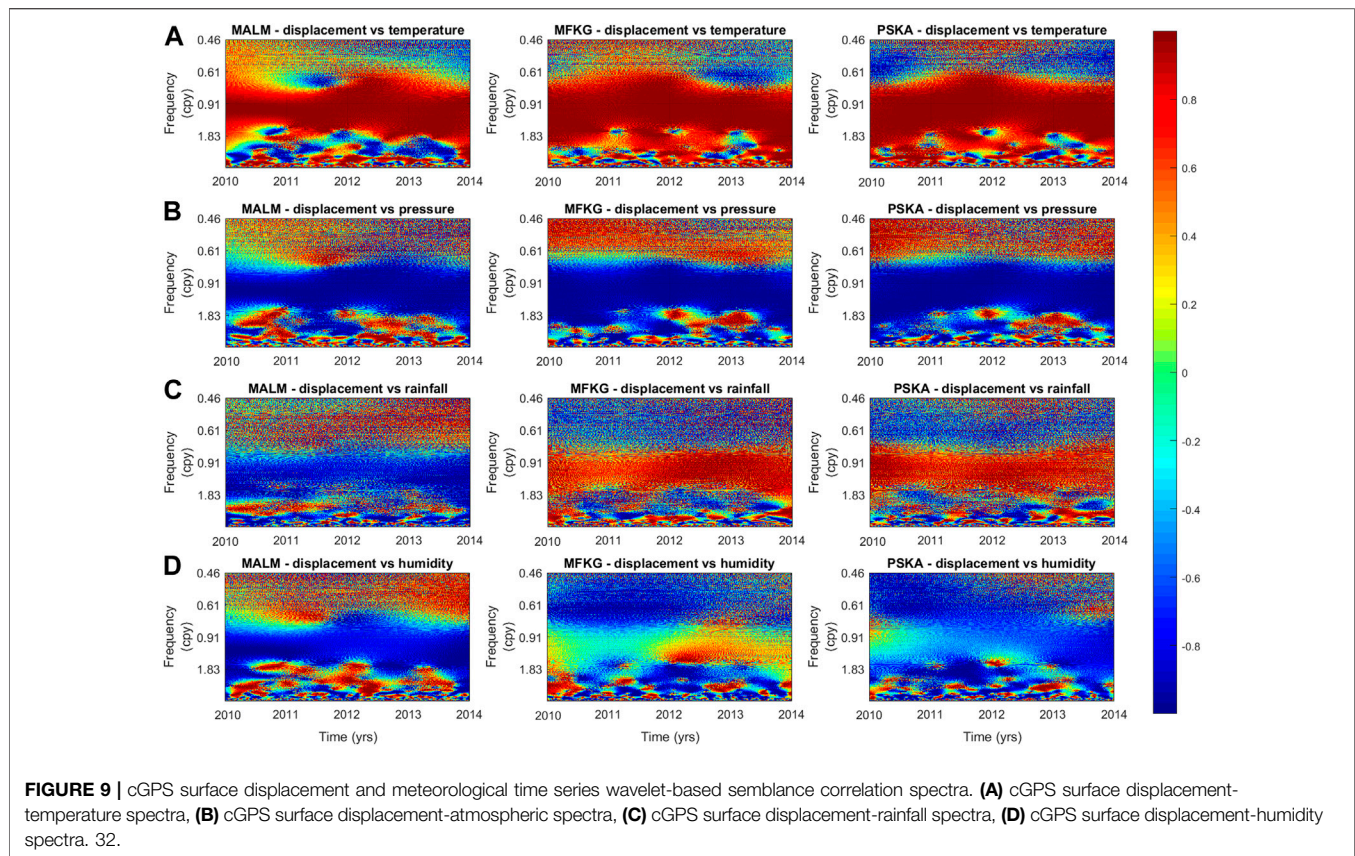
Meteorological Processes and Surface Displacement Relation

Generally, high temperatures cause thermal expansion of consolidated soil particles and water molecules in the near subsurface, expansion of the concrete and metallic components of the cGPS station, and the expansion of atmospheric air mass density (which results in a reduction in atmospheric pressure); all these phenomena may affect cGPS measurements. The opposite is thought to apply in cold conditions (i.e., winter), which might explain the high

correlation observed between atmospheric temperature, pressure, and vertical displacement changes.

The type of interaction (*viz.* reinforcement or opposition) between rainfall and humidity effects vs temperature and pressure effects on surface displacement is thought to vary spatially as postulated below:

- 1 In southern Africa's central and north-eastern parts, the rainfall-displacement and humidity-displacement time series are largely directly correlated. Thus, in summer, constructive interference may occur between rainfall and humidity surface deformation effects, with surface deformation effects induced by variations in atmospheric temperature and atmospheric pressure. Constructive interference may be occurring between surface deformation effects due to swelling on soil absorption of water and the seasonal tropospheric error introduced in the cGPS datasets due to high rainfall and humidity levels; with thermal expansion effects caused by thermal expansion of soil particles and water molecules in the near subsurface; and thermal expansion of concrete and metallic components of the cGPS stations in response to the prevalence of high temperatures and low atmospheric pressure.
- 2 In the south-western parts of southern Africa, the rainfall-displacement and humidity-displacements are anticorrelated.



Thus, in winter, destructive interference may occur between rainfall- and humidity-induced surface deformation effects, with surface deformation effect induced by variations in atmospheric temperature and atmospheric pressure. In addition, destructive interference may occur between surface deformation effects due to soil absorption of water molecules and the seasonal tropospheric error introduced in the cGPS datasets due to high rainfall and humidity levels, with thermal contraction effects due to the contraction of soil particles and water molecules in the near subsurface, and thermal contraction of concrete and metallic components of the cGPS stations in response to the prevalence of cold temperatures and high atmospheric pressure.

The spatially inconsistent and weak relationship between surface displacement, rainfall, and humidity processes observed from time, frequency, and time-frequency correlation is interpreted to imply that rainfall and humidity processes have little influence on seasonal surface displacement variations. Thus, deformation due to surficial hydrology (i.e., gravitational loading and soil consolidation induced by changes in surface and ground water levels) is also observed to have lesser influence on the seasonal surface displacement variations, the dominant factor is temperature. These findings are different to what has been found in other research studies and highlight the importance of carrying out thermal corrections (Wahr et al., 2004; Schmidt et al., 2006; Nahmani et al., 2012).

CONCLUSION

This study examines cGPS surface displacement and meteorological time series with the aim of improving their understanding and inferring the seasonal influence that the meteorological processes considered in this study have on surface displacement measurements measured by cGPS systems in southern Africa. Atmospheric temperature variations (thermoelastic effects) are found to have higher correlation with surface displacement time series, suggesting a greater thermal influence on the surface displacement measurements than water mass changes. These findings imply that correcting for thermal expansion effects in summer, thermal contraction in winter, and thermally-induced seasonal errors (thermoelastic effects) could reduce the seasonal variations observed in cGPS displacement time series in southern Africa and increase the accuracy of the cGPS displacement measurements. In turn, this could improve the accuracy of short-term crustal deformation measurements and their usefulness, for example, in the assessment of seismic hazard.

DATA AVAILABILITY STATEMENT

The datasets presented in this study can be found in online repositories. The names of the repository/repositories and accession number(s) can be found in the article/**Supplementary Material**.

AUTHOR CONTRIBUTIONS

SG wrote the manuscript under the supervision of GC, RD, and MM. All authors reviewed the final manuscript.

FUNDING

Council for Geoscience NRF through the South African Research Chairs Initiative (SARChI).

ACKNOWLEDGMENTS

We would like to acknowledge the Council for Geoscience and CIMERA for funding this research work, the South African Weather Service (SAWS), and TrigNet for providing the meteorological and availing the cGPS displacement data

REFERENCES

- Altamimi, Z., Rebischung, P., Métivier, L., Collilieux, X., and Baker, J. W. (2016). ITRF2014: A New Release of the International Terrestrial Reference Frame Modeling Nonlinear Station motions Quantitative Classification of Near-Fault Ground Motions Using Wavelet Analysis. *J. Geophys. Res. Solid Earth Bulletin Seismol. Soc. Am.* 12197, 61091486–61311501. doi:10.1785/012006025510.1002/2016jb013098
- Argus, D. F., Fu, Y., and Landerer, F. W. (2014). Seasonal Variation in Total Water Storage in California Inferred from GPS Observations of Vertical Land Motion. *Geophys. Res. Lett.* 41, 1971–1980. doi:10.1002/2014gl059570
- Baker, J. W. (2007). Quantitative classification of near-fault ground motions using wavelet analysis. *Bull. Seismol. Soc. Am.* 97, 1486–1501. doi:10.1785/0120060255
- Barry, R. G., and Chorley, R. J. (2010). *Atmosphere, Weather and Climate*. 9th edition. London, UK: Routledge Taylor & Francis Group.
- Blewitt, G., Hammond, W., and Kreemer, C. (2018). Harnessing the GPS Data Explosion for Interdisciplinary Science. *Eos* 99. doi:10.1029/2018EO104623
- Bollasina, M., and Nigam, S. (2010). The Summertime “Heat” Low over Pakistan/northwestern India: Evolution and Origin. *Clim. Dyn.* 37, 957–970. doi:10.1007/s00382-010-0879-y
- Byrne, M. P., Pendergrass, A. G., Rapp, A. D., and Wodzicki, K. R. (2018). Response of the Intertropical Convergence Zone to Climate Change: Location, Width, and Strength. *Curr. Clim. Change Rep.* 4, 355–370. doi:10.1007/s40641-018-0110-5
- Chase, B. M., and Meadows, M. E. (2007). Late Quaternary Dynamics of Southern Africa’s Winter Rainfall Zone. *Earth-Science Rev.* 84, 103–138. doi:10.1016/j.earscirev.2007.06.002
- Christensen, A. N. “Semblance Filtering of Airborne Potential Field Data,” in Proceedings of the Extended Abstracts, 16th ASEG Geophysical Conference and Exhibition, Adelaide, Australia, February 2003. (2003). doi:10.1071/aseg2003ab024
- Cilliers, P. J., Opperman, B. D. L., Mitchell, C. N., and Spencer, P. J. (2004). Electron Density Profiles Determined from Tomographic Reconstruction of Total Electron Content Obtained from GPS Dual Frequency Data: First Results from the South African Network of Dual Frequency GPS Receiver Stations. *Adv. Space Res.* 34, 2049–2055. doi:10.1016/j.asr.2004.08.002
- Cochran, W. T., Cooley, J. W., Favon, D. L., Helms, H. D., Kaenel, R. A., Lang, W. W., et al. (1967). What Is the Fast Fourier Transform? *Proc. IEEE* 55, 1664–1674. doi:10.1109/proc.1967.5957
- Cooper, G. R. J., and Cowan, D. R. (2008). Comparing Time Series Using Wavelet-Based Semblance Analysis. *Comput. Geosciences* 34, 95–102. doi:10.1016/j.cageo.2007.03.009

used to conduct the research. Special thanks go to the Department of Geophysics at the University of the Witwatersrand for providing the platform to carry out this work and its staff for providing constructive feedback on the work. RD acknowledges support from the NRF through the South African Research Chairs Initiative (SARChI). Some of the work presented here is part of the first author’s MSc thesis, titled: **Analysing ground surface position cGPS and meteorology measurements in southern Africa using signal processing techniques** (Gomo, 2019).

SUPPLEMENTARY MATERIAL

The Supplementary Material for this article can be found online at: <https://www.frontiersin.org/articles/10.3389/feart.2022.827011/full#supplementary-material>

- Cooper, G. R. J. (2009). Wavelet-based Semblance Filtering. *Comput. Geosciences* 35, 1988–1991. doi:10.1016/j.cageo.2008.10.017
- Davis, J. L., Elsegue, P., Mitrovica, J. X., and Tamisiea, M. E. (2004). Climate-driven Deformation of the Solid Earth from GRACE and GPS. *Geophys. Res. Lett.* 31, 1–4. doi:10.1029/2004GL021435
- Dong, D., Fang, P., Bock, Y., Cheng, K. M., and Miyazaki, S. (2002). Anatomy of Apparent Seasonal Variations from GPS-Derived Site Position Time Series. *J. Geophys. Res.* 107, 1–17. doi:10.1029/2001jb000573
- Ellis, J., and Galvin, K. A. (1994). Climate Patterns and Land-Use Practices in the Dry Zones of Africa, *BioScience* 44, 340–349. doi:10.2307/1312384
- Fletcher, P., and Sangwine, S. J. (2017). The Development of the Quaternion Wavelet Transform. *Signal Process.* 136, 2–15. doi:10.1016/j.sigpro.2016.12.025
- Friston, K. J., Bastos, A., Litvak, V., Stephan, K. E., Fries, P., and Moran, R. J. (2012). DCM for Complex-Valued Data: Cross-Spectra, Coherence and Phase-Delays. *NeuroImage* 59, 439–455. doi:10.1016/j.neuroimage.2011.07.048
- Fu, Y., Argus, D. F., Freymueller, J. T., and Heflin, M. B. (2013). Horizontal Motion in Elastic Response to Seasonal Loading of Rain Water in the Amazon Basin and Monsoon Water in Southeast Asia Observed by GPS and Inferred from GRACE. *Geophys. Res. Lett.* 40, 6048–6053. doi:10.1002/2013GL058093
- Gauthier, T. (2001). Detecting Trends Using Spearman’s Rank Correlation Coefficient. *Environ. Forensics* 2, 359–362. doi:10.1006/enfo.2001.0061
- Gomo, S. (2019). *Analysing Ground Surface Position cGPS and Meteorology Measurements in Southern Africa Using Signal Processing Techniques*. Johannesburg, Africa. University of the Witwatersrand. MSc dissertation
- Graps, A. (1995). An Introduction to Wavelets. *IEEE Comput. Sci. Eng.* 2, 50–61. doi:10.1109/99.388960
- He, X., Hua, X., Yu, K., Xuan, W., Lu, T., Zhang, W., et al. (2015). Accuracy Enhancement of GPS Time Series Using Principal Component Analysis and Block Spatial Filtering. *Adv. Space Res.* 55, 1316–1327. doi:10.1016/j.asr.2014.12.016
- Hepburn, H. R., and Radloff, S. E. (1998). *Honeybees of Africa*. Berlin, Germany. Springer-Verlag Berlin Heidelberg GmbH, United States of America. doi:10.1007/978-3-662-03604-4
- Hobbs, J. E., Lindesay, L. A., and Bridgman, H. A. (1998). *Climate of the Southern Continents: Present, Past and Future*. New York, NY, USA: John Wiley & Sons.
- Issartel, J., Bardainne, T., Gaillot, P., and Marin, L. (2015). The relevance of the cross-wavelet transform in the analysis of human interaction—a tutorial. *Frontiers in Psychology* 5, 1566. doi:10.3389/fpsyg.2014.01566
- Jury, M. R. (2013). Climate Trends in Southern Africa. *Sajs* 109, 1–11. doi:10.1590/sajs.2013/980
- Kaiser, G. (2011). *A Friendly Guide to Wavelets*. Basel, Switzerland. Birkhuser. doi:10.1007/978-0-8176-8111-1
- Knowles, L. A., Bennett, R. A., and Harig, C. (2020). Vertical Displacement of the Amazon Basin from GRACE and GPS. *J. Geophys. Res.* 125. doi:10.1029/2019JB018105

- MacKellar, N., New, M., and Jack, C. (2014). Observed and Modelled Trends in Rainfall and Temperature for South Africa: 1960-2010. *Sajs* 110, 1–13. doi:10.1590/sajs.2014/20130353
- Mallat, S. (1998). *A Wavelet Tour of Signal Processing*. New York: Academic Press.
- Mallat, S. (2009). *A Wavelet Tour of Signal Processing*. 3rd edition. Cambridge, MA, USA: Academic Press.
- Malservici, R., Hugentobler, U., Wonnacott, R., and Hackl, M. (2013). How Rigid Is a Rigid Plate? Geodetic Constraint from the TrigNet CGPS Network, South Africa. *Geophys. J. Int.* 192, 918–928. doi:10.1093/gji/ggs081
- Meyers, S. D., Kelly, B. G., and O'Brien, J. J. (1993). An Introduction to Wavelet Analysis in Oceanography and Meteorology: with Application to the Dispersion of Yanai Waves. *Mon. Wea. Rev.* 121, 2858–2866. doi:10.1175/1520-0493(1993)121<2858:aitwai>2.0.co;2
- Min, W., Zheng-Kang, S., and Da-Nan, D. (2005). The Effect and Correction of Non-tectonic Crustal Deformation and Continuous GPS Position Time Series. *Chin. J. Geophys.* 48, 1121–1129. doi:10.1002/cjg2.755
- Mukaka, M. M. (2012). Statistics Corner: A Guide to Appropriate Use of Correlation Coefficient in Medical Research. *Malawi Med. J.* 24, 69–71. doi:10.1016/j.cmpb.2016.01.020
- Nahmani, S., Bock, O., Bouin, M.-N., Santamaría-Gómez, A., Boy, J.-P., Collilieux, X., et al. (2012). Hydrological Deformation Induced by the West African Monsoon: Comparison of GPS, GRACE and Loading Models. *J. Geophys. Res.* 117, a–n. doi:10.1029/2011JB009102
- Nicholson, S. E., and Flohn, H. (1980). African Environmental and Climatic Changes and the General Atmospheric Circulation in Late Pleistocene and Holocene. *Clim. Change* 2, 313–348. doi:10.1007/bf00137203
- Potter, T. R., and Colman, B. R. (2003). *Handbook of Weather, Climate, and Water: Atmospheric Chemistry, Hydrology and Social Impacts*. Hoboken, NJ, USA: John Wiley & Sons.
- Rabbel, W., and Schuh, H. (1986). The Influence of Atmospheric Loading on VLBI-Experiments. *J. Geophys.* 59, 164–170.
- Ray, J., Altamimi, Z., Collilieux, X., and van Dam, T. (2008). Anomalous Harmonics in the Spectra of GPS Position Estimates. *GPS Solut.* 12, 55–64. doi:10.1007/s10291-007-0067-7
- Rebeschung, P., Altamimi, Z., Ray, J., and Garayt, B. (2016). The IGS Contribution to ITRF2014. *J. Geod.* 90, 611–630. doi:10.1007/s00190-016-0897-6
- Romagnoli, C., Zerbin, S., Lago, L., Richter, B., Simon, D., Domenichini, F., et al. (2003). Influence of Soil Consolidation and Thermal Expansion Effects on Height and Gravity Variations. *J. Geodyn.* 35, 521–539. doi:10.1016/S0264-3707(03)00012-7
- Ryan, O. (2015). Linear Algebra, Signal Processing, and Wavelets: a Unified Approach-MATLAB Version. Available from: <https://www.uio.no/studier/emner/matnat/math/nedlagte-emner/MAT-INF2360/v15/kompendium/applinalgmatlab.pdf>.
- Schmidt, R., Schwintzer, P., Flechtner, F., Reigber, C., Guntner, A., Doll, P., et al. (2006). GRACE Observations of Changes in Continental Water Storage. *Glob. Planet. Change* 50, 112–126. doi:10.1016/j.gloplacha.2004.11.018
- Struzik, Z. R. (2001). Wavelet Methods in (Financial) Time-Series Processing. *Phys. A Stat. Mech. its Appl.* 296, 307–319. doi:10.1016/s0378-4371(01)00101-7
- Sun, X., Cook, K. H., and Vizy, E. K. (2017). The South Atlantic Subtropical High: Climatology and Interannual Variability. *J. Clim.* 30, 3279–3296. doi:10.1175/JCLI-D-16-0705.1
- Teolis, A. (1998). *Computational Signal Processing with Wavelets*. Boston, MA, USA: Birkhuser Boston Inc.
- Torrence, C., and Compo, G. P. (1998). A Practical Guide to Wavelet Analysis. *Bull. Amer. Meteor. Soc.* 79, 61–78. doi:10.1175/1520-0477(1998)079<0061:apgtwa>2.0.co;2
- Trauth, M. H. (2010). *MATLAB Recipes for Earth Sciences*. 3rd edition. Berlin, Germany: Springer.
- van Dam, T. M., and Wahr, J. (1998). Modeling Environment Loading Effects: a Review. *Phys. Chem. Earth* 23, 1077–1087. doi:10.1016/S0079-1946(98)00147-5
- van Dam, T., Wahr, J., Milly, P. C. D., Shmakin, A. B., Blewitt, G., Lavallée, D., et al. (2001). Crustal Displacements Due to Continental Water Loading. *Geophys. Res. Lett.* 28, 651–654. doi:10.1029/2000gl012120
- Wahr, J., Swenson, S., Zlotnicki, V., and Velicogna, I. (2004). Time-variable Gravity from GRACE: First Results. *Geophys. Res. Lett.* 31, a–n. doi:10.1029/2004GL019779
- Warner, R. M. (1998). New York, NY, USA: Guilford Press, xiv. 225.
- Xu, X., Dong, D., Fang, M., Zhou, Y., Wei, N., and Zhou, F. (2017). Contributions of Thermoelastic Deformation to Seasonal Variations in GPS Station Position. *GPS Solut.* 21, 1265–1274. doi:10.1007/s10291-017-0609-6
- Yan, H., Chen, W., Zhu, Y., Zhang, W., and Zhong, M. (2009). Contributions of Thermal Expansion of Monuments and Nearby Bedrock to Observed GPS Height Changes. *Geophys. Res. Lett.* 36, 1–5. doi:10.1029/2009GL038152
- Zhao, G., Jiang, D., Diao, J., and Qian, L. (2004). “Application of Wavelet Time-Frequency Analysis on Fault Diagnosis for Steam Turbine,” in Proceedings of the Surveillance 5 CETIM, Senlis, France, October 2004, 11–13

Conflict of Interest: The authors declare that the research was conducted in the absence of any commercial or financial relationships that could be construed as a potential conflict of interest.

Publisher’s Note: All claims expressed in this article are solely those of the authors and do not necessarily represent those of their affiliated organizations, or those of the publisher, the editors and the reviewers. Any product that may be evaluated in this article, or claim that may be made by its manufacturer, is not guaranteed or endorsed by the publisher.

Copyright © 2022 Gomo, Cooper, Durrheim and Manzi. This is an open-access article distributed under the terms of the Creative Commons Attribution License (CC BY). The use, distribution or reproduction in other forums is permitted, provided the original author(s) and the copyright owner(s) are credited and that the original publication in this journal is cited, in accordance with accepted academic practice. No use, distribution or reproduction is permitted which does not comply with these terms.